© 2017. Published by The Company of Biologists Ltd | Development (2017) 144, 3789-3797 doi:10.1242/dev.153353

RESEARCH ARTICLE

HDAC3 promotes meiotic apparatus assembly in mouse oocytes by modulating tubulin acetylation

Xiaoyan Li[1], Xiaohui Liu[1], Min Gao[1], Longsen Han[2], Danhong Qiu[2], Haichao Wang[2], Bo Xiong[1], Shao-Chen Sun[1], Honglin Liu[1] and Ling Gu[1,*]

ABSTRACT

Histone deacetylases (HDACs) have been shown to deacetylate numerous cellular substrates that govern a wide array of biological processes. HDAC3, a member of the Class I HDACs, is a highly conserved and ubiquitously expressed protein. However, its roles in meiotic oocytes are not known. In the present study, we find that mouse oocytes depleted of HDAC3 are unable to completely progress through meiosis, and are blocked at metaphase I. These HDAC3 knockdown oocytes show spindle/chromosome organization failure, with severely impaired kinetochore-microtubule attachments. Consistent with this, the level of BubR1, a central component of the spindle assembly checkpoint, at kinetochores is dramatically increased in metaphase oocytes following HDAC3 depletion. Knockdown and overexpression experiments reveal that HDAC3 modulates the acetylation status of α-tubulin in mouse oocytes. Importantly, the deacetylation mimetic mutant tubulin-K40R can partly rescue the defective phenotypes of HDAC3 knockdown oocytes. Our data support a model whereby HDAC3, through deacetylating tubulin, promotes microtubule stability and the establishment of kinetochore-microtubule interaction, consequently ensuring proper spindle morphology, accurate chromosome movement and orderly meiotic progression during oocyte maturation.

KEY WORDS: Oocyte, Meiosis, Cytoskeleton, Chromosome, Reproduction, Bub1b

INTRODUCTION

Acetylation of the lysine ε-amino group is a dynamic post-translational modification regulated by the opposing activities of lysine acetyltransferases and histone deacetylases (HDACs) (Seto and Yoshida, 2014; Zhan et al., 2017). To date, the HDAC family includes 18 members divided into Class I (HDACs 1-3 and 8), Class II (HDACs 4-7 and 9, 10), Class III (Sirt1-7) and Class IV (HDAC11) (Horiuchi et al., 2009). Class I, II and IV HDACs are zinc-dependent enzymes collectively referred to as classical HDACs, whereas Class III HDACs, commonly referred to as Sirtuins, require NAD^+ for their activity (Haberland et al., 2009; Yang and Seto, 2008). HDACs, as a vast family of enzymes, have been reported to play crucial roles in diverse biological processes, largely through their effects on transcription and chromatin conformation. Among them, Class I HDACs are ubiquitously expressed nuclear enzymes and conserved in a wide range of species (Mahlknecht et al., 1999; Vidal and Gaber, 1991; Yang et al., 1997). Conditional targeting of HDAC1 and HDAC2 in mice has been shown to lead to female infertility (Ma et al., 2012). In particular, HDAC2 regulates chromosome segregation and kinetochore function via H4K16 deacetylation during oocyte maturation (Ma and Schultz, 2013). In addition, HDAC6 appears to be an essential factor modulating oocyte maturation and meiotic apparatus assembly (Ling et al., 2017; Zhou et al., 2017). HDAC3 is required for the proliferation of adult neural stem/progenitor cells by modulating cyclin-dependent kinase levels (Jiang and Hsieh, 2014). HDAC3 was found to localize to the mitotic spindle of HeLa cells and participate in the establishment of interactions between kinetochore and microtubules (Ishii et al., 2008). Recently, it has shown that deletion of HDAC3 in adult beta cells improves glucose tolerance via increased insulin secretion (Remsberg et al., 2017). However, the function of HDAC3 in meiosis remains unknown.

Poor oocyte quality is a major cause of female infertility. In mammals, oocytes are arrested within ovarian follicles at the diplotene stage of the first meiotic prophase, which is also called germinal vesicle (GV) stage. These fully grown oocytes resume meiosis upon hormone stimulation. During this process, accurate control of spindle assembly and chromosome movement is essential for producing a healthy oocyte. Kinetochores provide the principal attachment of chromosomes to microtubules, while spindle assembly checkpoint (SAC) is the mechanism that monitors and responds to kinetochore-microtubule interaction. Unfaithful chromosome segregation during meiosis could lead to aneuploidy in the oocyte. Egg aneuploidy is a leading cause of spontaneous abortions, birth defects and developmental disabilities in humans (Ma et al., 2014). Although numerous molecules have been proposed to affect spindle/chromosome organization in oocyte meiosis, the underlying pathways that regulate the meiotic structure remain to be explored.

In the present study, we investigated the potential roles of HDAC3 in mouse oocytes by knockdown and overexpression assays. Our results indicate that HDAC3 depletion adversely influences meiotic maturation, especially spindle assembly and chromosome organization.

RESULTS

Localization of HDAC3 during oocyte maturation

To explore the role of HDAC3 in meiosis, we first examined its distribution at different stages of the mouse oocyte by immunostaining and confocal microscopy. HDAC3 is predominantly distributed in the nucleus of GV oocytes (Fig. 1A, arrowhead). However, accompanying meiotic resumption, HDAC3 resides in the cytoplasm, with signals accumulating on the meiotic spindle region from pre-metaphase I to metaphase II. Double staining was performed to confirm the spatial relationship between

[1]College of Animal Science & Technology, Nanjing Agricultural University, 210095 Nanjing, China. [2]State Key Laboratory of Reproductive Medicine, Nanjing Medical University, 211166 Nanjing, China.

*Author for correspondence (lgu@njau.edu.cn)

L.H., 0000-0001-9951-4156; D.Q., 0000-0001-9661-2105; H.W., 0000-0002-0149-9240; L.G., 0000-0002-3368-4053

Received 19 April 2017; Accepted 30 August 2017

Development (2017) 144, 3789-3797 doi:10.1242/dev.153353

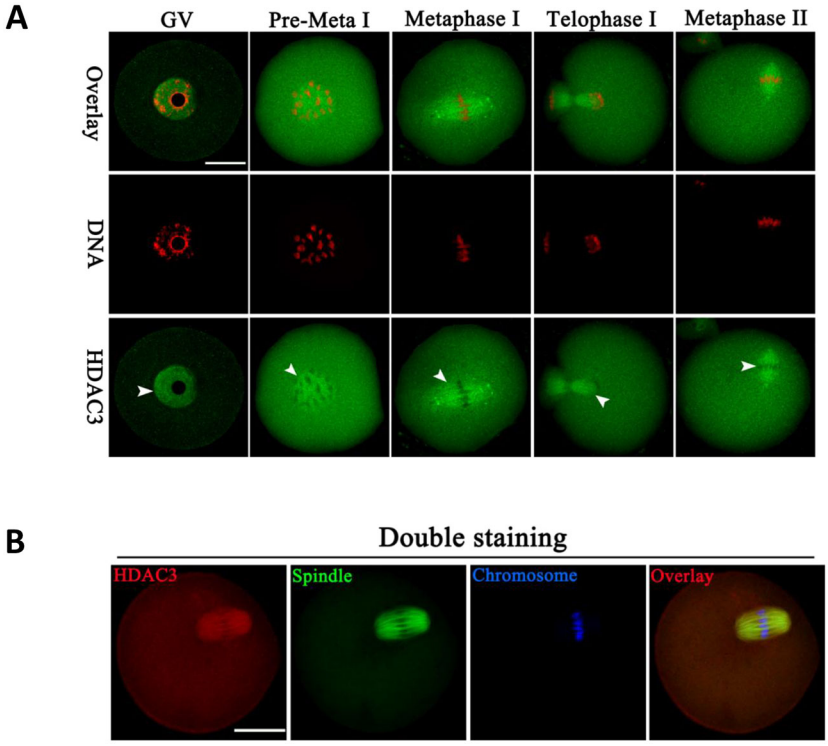

Fig. 1. Localization of HDAC3 during mouse oocyte maturation. (A) Mouse oocytes at GV, pre-metaphase I, metaphase I, telophase I and metaphase II were immunolabeled with HDAC3 antibody (green) and counterstained with PI to visualize DNA (red). Arrowheads indicate the accumulated HDAC3 signal. (B) Double labeling of metaphase oocytes with HDAC3 antibody (green) and α-tubulin antibody (red), and counterstaining of DNA with Hoechst 33342 (blue). Scale bars: 30 µm.

HDAC3 and the spindle. HDAC3 is indeed colocalized with the meiotic spindle in mouse oocytes, as evidenced by the overlapping fluorescence signals (Fig. 1B). In addition, to confirm whether the HDAC3 antibody staining pattern is specific, exogenous Myc-HDAC3 was ectopically expressed in mouse oocytes, and then metaphase cells were labeled with anti-Myc antibody. Myc-HDAC3 is distributed in the cytoplasm, with strong signals on the spindle region (Fig. S1, arrowheads), similar to the localization of endogenous HDAC3 protein.

HDAC3 knockdown adversely affects mouse oocyte maturation

The progression of oocyte maturation includes meiotic resumption indicated by germinal vesicle breakdown (GVBD), microtubule organization in meiosis I (MI), extrusion of the first polar body (Pb1), and then progression to metaphase II (MII) in preparation for fertilization. To explore the role of HDAC3, fully grown oocytes were microinjected with specifically designed HDAC3 siRNAs, with a negative siRNA injected as control. After injection, the oocytes were arrested at GV stage for 20 h with milrinone to degrade mRNA. Based on western blotting results, we found that siRNA #2 led to the most substantial reduction in HDAC3 protein in oocytes (Fig. 2A). qRT-PCR assay confirmed that siRNA #2 could efficiently decrease endogenous *Hdac3* mRNA levels in mouse oocytes (Fig. 2B). Similarly, siRNA knockdown also resulted in a significant decrease in HDAC3 immunofluorescent signal in oocytes (Fig. S2). Therefore, siRNA #2 was used in subsequent knockdown experiments. Of note, we found that the siRNA-injected oocytes displayed wide variation in HDAC3 staining (see images I and II in Fig. S2), which might contribute to distinct oocyte phenotypes (see below).

After 3 h of culture, both control and HDAC3 knockdown (KD) oocytes resumed meiosis normally, as evidenced by the similar GVBD rate (Fig. 2D). However, only 42.5% of HDAC3 KD oocytes extruded Pb1 after 14 h of culture, a significant decrease compared with controls (Fig. 2C arrowheads, 2E). In addition, a high frequency of HDAC3 KD oocytes underwent symmetric division, displaying the '2-cell like' phenotype (Fig. 2C, asterisks). Specifically, nuclear staining and quantitative analysis revealed that 39.8% of HDAC3 KD oocytes were arrested at MI, which was significantly higher than that of control oocytes (Fig. 2F). To examine why the rest of the oocytes are still able to progress through meiosis, HDAC3 staining was performed on siRNA-injected oocytes with or without Pb1. As shown in Fig. S3, HDAC3 intensity was significantly higher in MII oocytes than in MI-arrested oocytes, indicating that the different phenotypes are associated with the degree of HDAC3 depletion. These observations strongly suggest that HDAC3 is required for orderly oocyte maturation and meiotic divisions.

Proper spindle formation and chromosome alignment require HDAC3

The specific distribution of HDAC3 on the spindle and its effects on maturation progression prompted us to investigate whether HDAC3 depletion in oocytes influences the meiotic apparatus. Control and HDAC3 KD oocytes were immunolabeled with anti-tubulin antibody to visualize the spindle and counterstained with propidium iodide (PI) to visualize chromosomes. Significantly, HDAC3 KD elevated the percentage of spindle defects and chromosome misalignment in metaphase oocytes (Fig. 3A,B), which showed elongated/multipolar spindles (arrows) and scattered chromosomes (arrowheads). These phenotypes contrasted sharply with control oocytes showing the typical barrel-shaped spindle and well-aligned chromosomes at the equator. Together, these findings indicate that HDAC3 KD oocytes are unable to properly assemble the spindle and align the chromosomes in meiosis.

HDAC3 KD impairs kinetochore-microtubule attachments

Accurate chromosome alignment and segregation depend on the proper attachment of kinetochores to microtubules emanating from

Development (2017) 144, 3789-3797 doi:10.1242/dev.153353

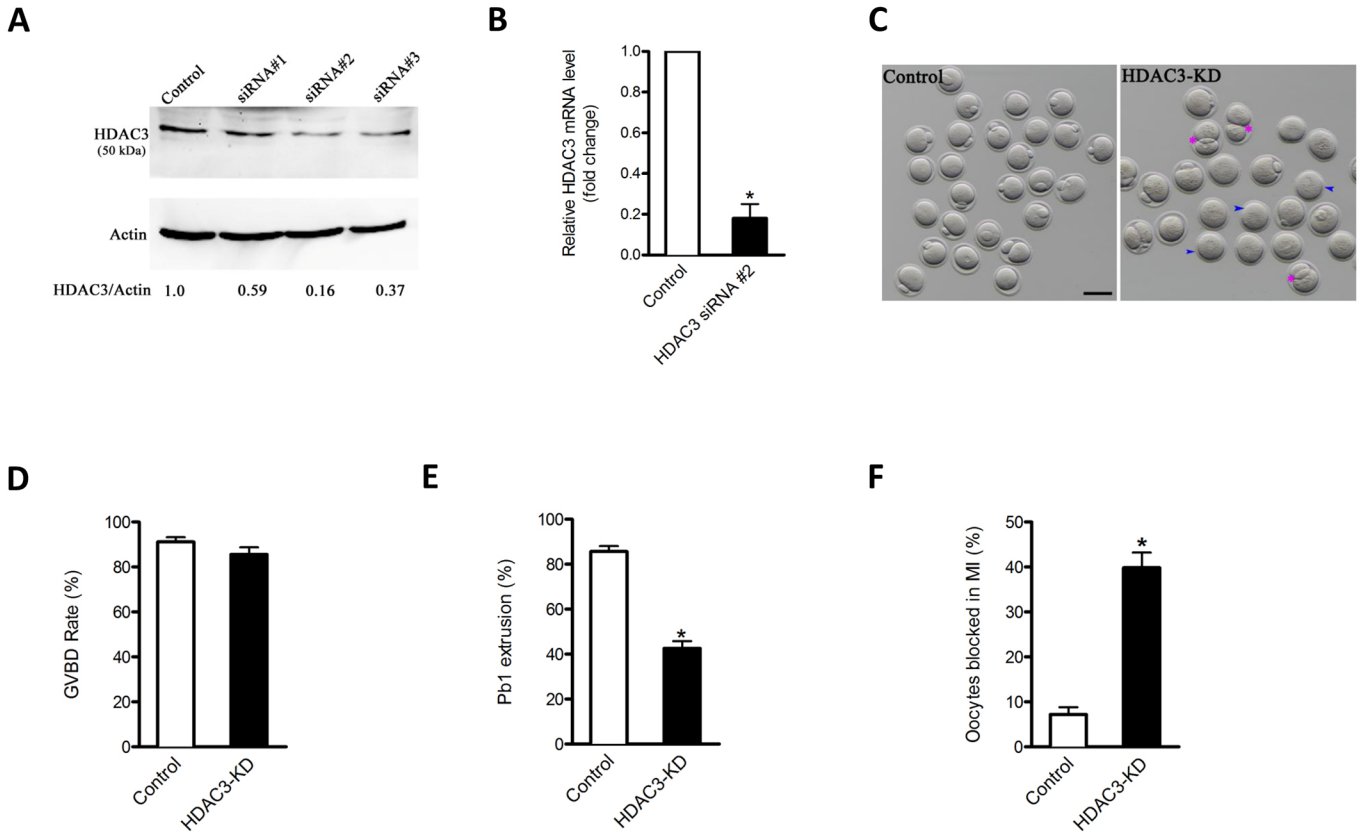

Fig. 2. Effects of HDAC3 knockdown on oocyte maturation. Fully grown oocytes were microinjected with HDAC3 siRNAs, then arrested at GV stage with milrinone to promote mRNA degradation. (A) Knockdown (KD) of endogenous HDAC3 protein after HDAC3 siRNA injection was confirmed by western blot. (B) The efficiency of HDAC3 siRNA-mediated KD was verified by qRT-PCR. (C) Phase-contrast images of control and HDAC3 siRNA-injected oocytes. Asterisks denote oocytes with apparent symmetrical division and arrowheads indicate oocytes that fail to extrude polar bodies. Scale bar: 80 µm. (D,E) Quantitative analysis of GVBD rate and Pb1 extrusion rate of control (n=180) and HDAC3 KD (n=178) oocytes. (F) The percentage of meiosis I-arrested oocytes after HDAC3 siRNA injection. Mean±s.d. of the results obtained in three independent experiments. *P<0.05 versus control.

opposite spindle poles (Tauchman et al., 2015). Given the spindle/chromosome disorganization in HDAC3 KD oocytes, we examined whether kinetochore-microtubule (K-MT) attachments were compromised correspondingly. MI oocytes were labeled with CREST (also known as Ss18l1) antibody to detect kinetochores, with anti-tubulin antibody to visualize spindle, and co-stained with Hoechst 33342 for chromosomes (Fig. 4A). We found that the majority of normal oocytes presented amphitelic K-MT attachments (every kinetochore attached to one pole; chromosomes labeled 1 and 2 in Fig. 4A,B). By contrast, the frequency of K-MT misattachments in HDAC3 KD oocytes was greatly increased relative to control cells, including lost attachments (kinetochore

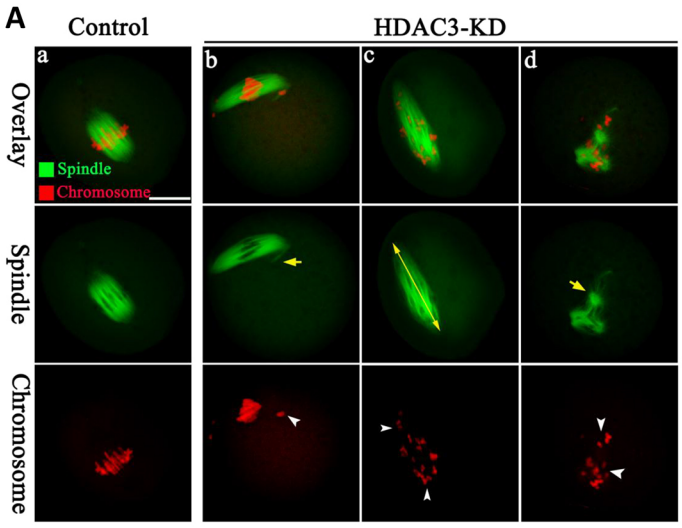

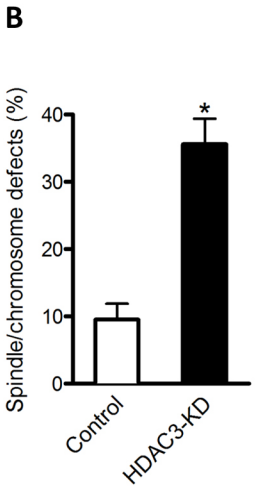

Fig. 3. HDAC3 KD causes spindle defects and chromosome misalignment in oocyte meiosis. (A) Control and HDAC3 KD oocytes were stained with α-tubulin antibody to visualize spindle (green) and counterstained with PI to visualize chromosomes (red). (a) Control oocytes showing the characteristic barrel-shaped spindle and well-aligned chromosomes. (b-d) Three examples illustrating the elongated and disorganized spindles (arrows) and misaligned chromosomes (arrowheads) that were frequently observed in HDAC3 KD oocytes. Scale bar: 30 µm (B) Quantification of control (n=136) and HDAC3 KD (n=152) oocytes with spindle/chromosome defects. Mean percentage± s.d. of three independent experiments. *P<0.05 versus control.

Development (2017) 144, 3789-3797 doi:10.1242/dev.153353

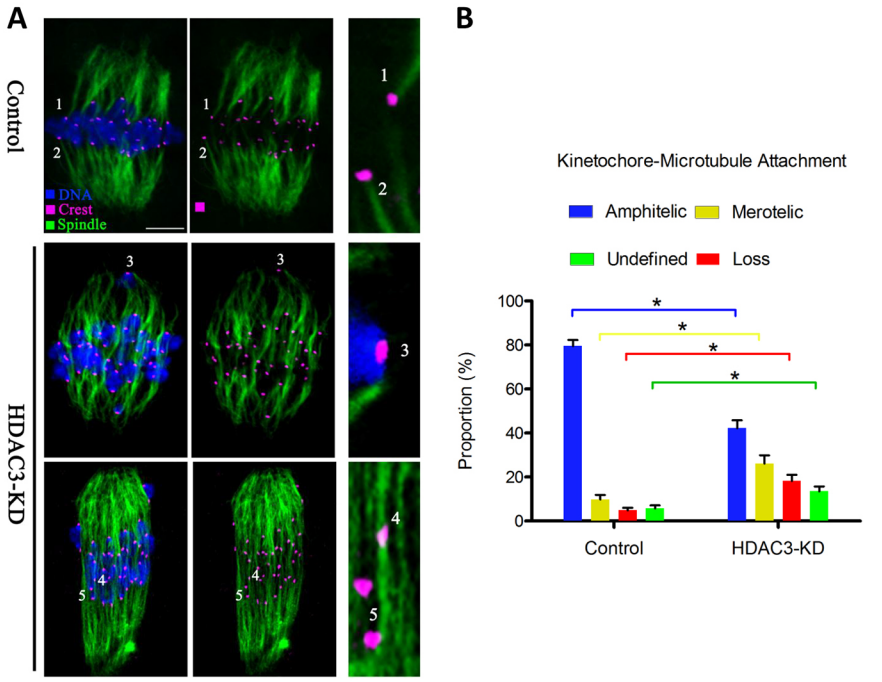

Fig. 4. HDAC3 KD impairs kinetochore-microtubule (K-MT) attachments during oocyte meiosis. (A) Control and HDAC3 KD metaphase oocytes were labeled with CREST antibody for kinetochores (purple), anti-tubulin antibody for microtubules (green) and Hoechst 33342 for chromosomes (blue). Representative confocal images are shown. Chromosomes labeled 1 and 2 represent examples of amphitelic attachment, chromosome 3 represents lost attachment, chromosome 4 represents merotelic attachment, and chromosome 5 represents undefined attachment. (B) Quantitative analysis of K-MT attachments in control and HDAC3 KD oocytes. Kinetochores in regions where fibers were not easily visualized were not included in the analysis. 13 control oocytes and 11 HDAC3 KD oocytes were examined. *P<0.05 versus controls.

attached to neither of the poles; chromosome 3), merotelic attachment (one kinetochore attached to both poles; chromosome 4), as well as undefined attachment (chromosome 5). These erroneous K-MT attachments are likely to be the major factor contributing to the chromosome alignment failure observed in HDAC3 KD oocytes, influencing the establishment of stable chromosome biorientation.

HDAC3 KD activates the SAC

The SAC is a ubiquitous safety device that monitors K-MT interactions and ensures accurate chromosome segregation (Overlack et al., 2015). Once the K-MT attachments are disturbed, the anaphase-inhibitory signal is triggered by the SAC (Tauchman et al., 2015). Taking into account the impaired K-MT attachments and MI arrest in HDAC3 KD oocytes, we proposed that the SAC might be provoked when HDAC3 is depleted. To test this, control and HDAC3 KD oocytes were immunolabeled for BubR1 (also known as Bub1b), an integral component of the checkpoint complex, to evaluate SAC activity. In control cells, BubR1 was detected on unattached kinetochores during pre-metaphase, and then completely disappeared once kinetochores had become properly attached to microtubules at metaphase I (Fig. 5). Remarkably, the BubR1 signal on kinetochores was dramatically increased in those HDAC3 KD oocytes arrested at MI (Fig. 5A,B, arrowhead), implying that SAC was activated. Collectively, these findings suggest that the SAC surveillance mechanism might be a major pathway mediating the effects of HDAC3 KD on meiotic progression in oocytes.

Incidence of aneuploidy is increased in HDAC3 KD oocytes

In normal cells, SAC delays anaphase onset until all chromosomes are well aligned at the equatorial plane and attached to the spindle

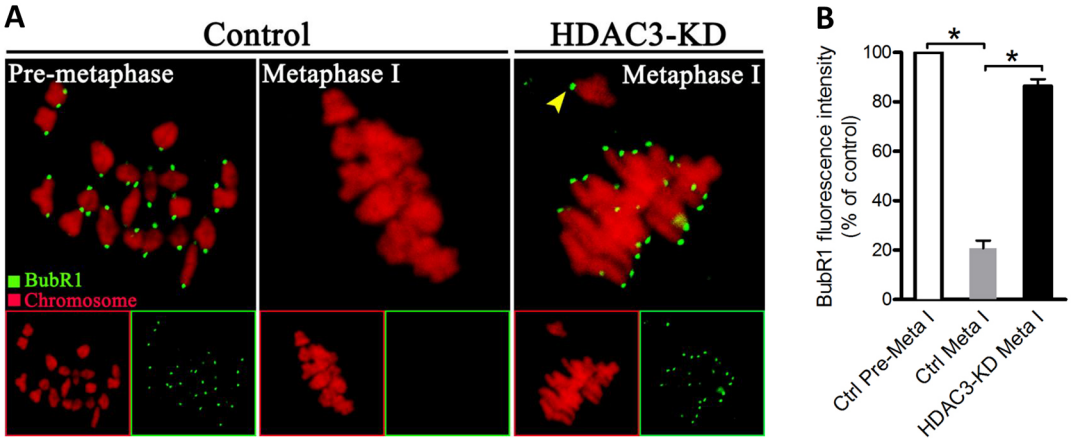

Fig. 5. HDAC3 KD activates the SAC during oocyte meiosis. (A) Control and HDAC3 KD oocytes were immunolabeled with anti-BubR1 antibody (green) and counterstained with PI to examine chromosomes (red). Representative confocal images of pre-metaphase I and metaphase I oocytes are shown. Arrowhead indicates a scattered chromosome in HDAC3 KD oocytes. (B) Quantification of BubR1 fluorescence intensity in control (n=25) and HDAC3 KD (n=26) oocytes. Mean percentage±s.d. of three independent experiments. *P<0.05 versus controls.

Development (2017) 144, 3789-3797 doi:10.1242/dev.153353

apparatus. Dysregulated SAC is thought to be the major driving force of aneuploidy generation. Because of the high frequency of spindle/chromosome defects in HDAC3 KD oocytes, we examined whether the incidence of aneuploidy was accordingly increased. MII oocytes were processed for chromosome spreading and kinetochore labeling. Representative images of euploidy and aneuploidy are shown in Fig. 6A. Quantitative analysis (Fig. 6B) further revealed that HDAC3 KD resulted in a ∼3- to 4-fold increase in the incidence of aneuploidy eggs compared with controls. To confirm this karyotypic phenotype, we also counted chromosome number using a monastrol-based *in situ* spreading technique (Duncan et al., 2009; Lane et al., 2010), and similar results were obtained (Fig. S4). These findings suggest that HDAC3 KD disrupts spindle/chromosome organization and provokes SAC during meiosis, which in turn elevates the incidence of aneuploidy.

HDAC3 controls spindle/chromosome organization in oocytes by maintaining the hypoacetylation state of tubulin

Tubulin is one of the most abundant non-histone proteins subject to acetylation, which occurs on lysine 40 of the α-tubulin subunit (Zilberman et al., 2009). Tubulin acetylation was first identified in flagellar axonemes of *Chlamydomonas reinhardtii* (Eddé et al., 1991). Subsequent studies demonstrated that this modification is also present in basal bodies and a subset of cytoplasmic microtubules (Piperno et al., 1987). Furthermore, tubulin acetylation was shown to be mainly on stable microtubules resistant to depolymerization induced by cold shock (Li and Yang, 2015). Of note, HDAC3 is able to modulate tubulin acetylation in a human prostate cancer cell line (Bacon et al., 2015). Hence, the involvement of HDAC3 in meiotic apparatus assembly prompted us to consider tubulin as a potential target mediating this process.

We found that the acetylation levels of α-tubulin were dramatically increased in HDAC3 KD mouse oocytes as compared with controls, whereas overexpression of HDAC3 significantly reduced the fluorescence intensity of acetylated tubulin (Fig. 7A,B). These results indicate that the acetylation status of tubulin depends on HDAC3 expression in mouse oocytes.

It has been shown that the substitution of lysine (K) with glutamine (Q) mimics an acetylated amino acid state, whereas substitution with arginine (R) mimics deacetylation (Gal et al., 2013; Zhang et al., 2015). To investigate whether tubulin acetylation affects meiotic structure in oocytes, we constructed site-specific mutants (K-to-Q and K-to-R) targeting lysine 40 (K40) of tubulin. The mRNA encoding these tubulin mutants was microinjected into oocytes and the effects on spindle/chromosome organization evaluated. As shown in Fig. 8A,B, tubulin-K40Q resulted in an almost 3-fold increase in the incidence of spindle/chromosome defects compared with the unmutated tubulin (tubulin-WT) control. Moreover, tubulin-K40Q also efficiently induced activation of the SAC in meiosis as compared with the tubulin-K40R mutant (Fig. 8C,D). These observations suggest that tubulin acetylation is essential for spindle assembly and chromosome congression in meiotic oocytes.

Finally, we asked whether the non-acetylatable mimetic mutant of tubulin could rescue at least some of the phenotypic defects seen in HDAC3 KD oocytes. Tubulin-K40R was microinjected into HDAC3 KD oocytes and mature oocytes were then stained to evaluate spindle/chromosome organization. Tubulin-K40R significantly lowered the proportion of abnormal spindle/chromosomes in HDAC3 KD oocytes (Fig. 8E,F). These results suggest that non-acetylated tubulin-K40R is capable, at least in part, of preventing the meiotic defects that arise in the oocyte as a result of HDAC3 loss.

Taken together, we conclude that HDAC3 controls assembly of the meiotic apparatus in oocytes by maintaining the hypoacetylation state of tubulin.

DISCUSSION

HDAC3 is a crucial epigenetic modifying enzyme and regulator of the maintenance of chromatin structure and genome stability, ensuring normal cell viability (Bhaskara et al., 2010; Takami and Nakayama, 2000). In this study, we showed that HDAC3 predominantly accumulates on the spindle accompanying meiotic resumption (Fig. 2), which is in line with previous findings in somatic cells (Ishii et al., 2008). In support of this observation, we further discovered that HDAC3 KD in oocytes disrupts spindle assembly and chromosome alignment and impairs K-MT interaction. K-MT linkage is essential for the poleward chromosome movement in meiosis. The kinetochore is composed of a number of conserved protein complexes that assemble on the centromere, a specialized chromatin domain (Santaguida and Musacchio, 2009). The correct chromosome alignment to the metaphase plate requires bipolar attachment and tension between kinetochore and microtubule. It is therefore

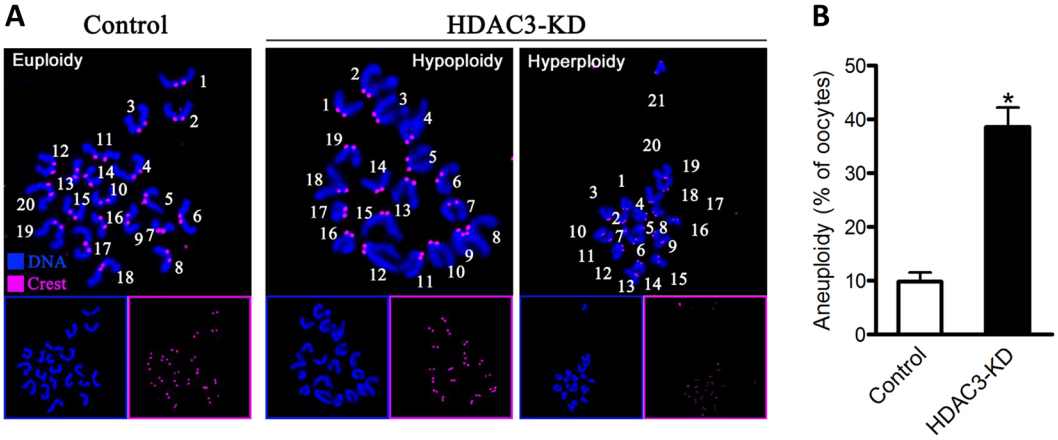

Fig. 6. HDAC3 KD increase the incidence of aneuploidy in mouse oocytes. (A) Chromosome spread of control and HDAC3 KD oocytes. Chromosomes were stained with Hoechst 33342 (blue) and kinetochores were labeled with CREST antibody (purple). Representative confocal images show euploid control oocytes and aneuploid HDAC3 KD oocytes. (B) Quantification of aneuploidy in control (n=40) and HDAC3 KD (n=43) oocytes. Mean percentage±s.d. of three independent experiments. *P<0.05 versus controls.

Development (2017) 144, 3789-3797 doi:10.1242/dev.153353

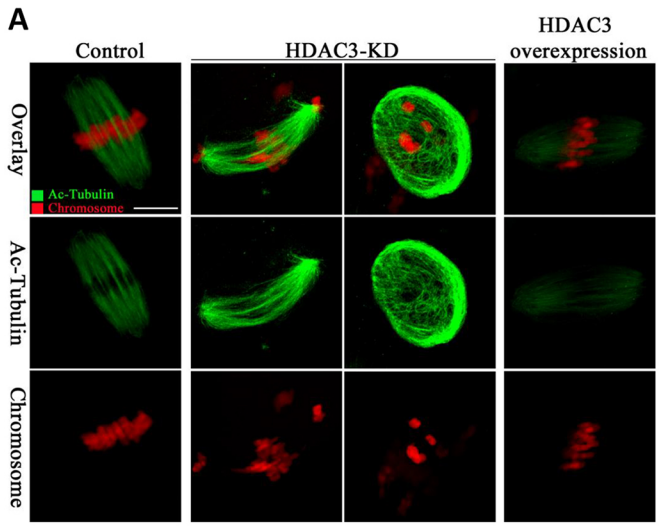

Fig. 7. HDAC3 modulates the acetylation state of α-tubulin in mouse oocytes. (A) Metaphase oocytes were immunolabeled with acetylated α-tubulin antibody (green) and counterstained with PI to show chromosomes (red). Representative confocal images are shown of acetylated tubulin in control, HDAC3 KD and HDAC3 overexpression oocytes. (B) Quantification of fluorescence intensity of acetylated tubulin in control (n=20), HDAC3 KD (n=18) and HDAC3 overexpression (OE) (n=21) oocytes. Mean percentage±s.d. of three independent experiments. *P<0.05 versus controls. Scale bars: 10 µm.

conceivable that the high percentage of spindle/chromosome abnormalities in HDAC3 KD oocytes is a consequence of K-MT misattachments. These attachment errors need be corrected in normal cells; otherwise, they would cause chromosome separation defects if they persisted until anaphase. Consistent with this notion, the frequency of aneuploidy was significantly increased in HDAC3-depleted oocytes relative to controls (Fig. 6). We propose that, in HDAC3 KD oocytes, compromised K-MT stability and the resulting meiotic defects contribute to the generation of aneuploid eggs observed in our experiments.

Regulation of microtubule dynamics and organization is essential for bipolar spindle assembly and function. Microtubules are essential cytoskeletal polymers that are made of repeating α/β-tubulin heterodimers (Nogales, 2000). Tubulin is one of the most abundant non-histone proteins subject to acetylation. It is worth noting that α-tubulin acetylation serves as a marker for the presence of stable microtubules and affects the activity of microtubule-associated proteins and microtubule-based motors (Chen et al., 2013). Acetylated microtubules have been detected in mouse oocytes (Schatten et al., 1988); however, their function(s) during meiosis remains unknown. Here, by constructing site-specific mutants targeting tubulin K40, we demonstrated that tubulin acetylation is essential for spindle assembly and chromosome congression in meiotic oocytes (Zhan et al., 2017) (Fig. 7). HDAC3 has been shown to indirectly modulate tubulin acetylation in human prostate cancer cells (Bacon et al., 2015). In our study, we observed the enrichment of HDAC3 protein on the spindle during oocyte maturation. Moreover, as revealed by our knockdown and overexpression experiments (Fig. 7), HDAC3 evidently controls the acetylation level of α-tubulin in oocytes. Hence, the evidence strongly suggests that α-tubulin may be an important deacetylation target of HDAC3 in mouse oocytes. Interestingly, recent reports show that treatment with tubastatin A, an HDAC6 inhibitor, also increases the acetylation level of α-tubulin in mouse oocytes (Ling et al., 2017; Zhou et al., 2017). It remains to be determined how α-tubulin hyperacetylation disrupts spindle assembly and chromosome movement during oocyte meiosis, potentially through affecting microtubule stability and K-MT interaction. Combined with our tubulin-K40R rescue experiments (Fig. 8), these data lead us to propose that HDAC3 depletion induces tubulin hyperacetylation, which in turn compromises microtubule stability and K-MT attachments, leading to spindle/chromosome organization failure and aneuploidy. Our data cannot exclude the possibility that HDAC3 might act on other targets in its function during oocyte maturation. Owing to the limitation in oocyte number and for technical reasons, we have not been able to analyze the relationship between α-tubulin acetylation and its stability in mouse oocytes. Further assays will be required to clarify these issues.

The proportion of MI-arrested oocytes was significantly increased by HDAC3 KD (Fig. 2). The kinetochore has been shown to function as a signaling hub that coordinates chromosome attachment, SAC activity, and cell cycle progression from metaphase to anaphase. In the presence of unattached kinetochores, SAC proteins form a complex that inhibits anaphase onset (Tauchman et al., 2015). By confocal microscopy, we found that the BubR1 signal persists at metaphase chromosomes in HDAC3 KD oocytes compared with controls (Fig. 5). Interestingly, tubulin-K40R mutant expression was able to partly rescue these phenotypes in HDAC3 KD oocytes (Figs 7, 8). Considering the frequent K-MT misattachments, we reasoned that a metaphase-anaphase transition block arises in HDAC3 KD oocytes from the SAC activation.

In summary, we have discovered a novel pathway through which HDAC3 modulates the meiotic apparatus in oocytes. Our data support a model whereby HDAC3, most likely through deacetylating tubulin, promotes the establishment of K-MT interactions, consequently ensuring proper spindle morphology and accurate chromosome movement during oocyte maturation.

MATERIALS AND METHODS

Reagents

All chemicals and culture media were purchased from Sigma unless stated otherwise.

Mice

Female 4-week-old ICR mice (Charles River Laboratories China, Beijing, China) were used in all experiments. Experiments were approved by the Animal Care and Use Committee of Nanjing Agricultural University and were performed in accordance with institutional guidelines.

Antibodies

Primary antibodies: rabbit polyclonal anti-HDAC3 antibodies (Santa Cruz Biotechnology, sc-376957; 1:150); goat polyclonal anti-BubR1 (ab28193) and mouse monoclonal anti-Myc tag (ab18185) antibodies (Abcam; 1:250); mouse polyclonal anti-acetylated tubulin (Lys 40) (Sigma, T7451; 1:200); human anti-centromere CREST antibody (Antibodies Incorporated, 15-234; 1:500); mouse monoclonal anti-α-tubulin (A5441) and FITC-conjugated

Development (2017) 144, 3789-3797 doi:10.1242/dev.153353

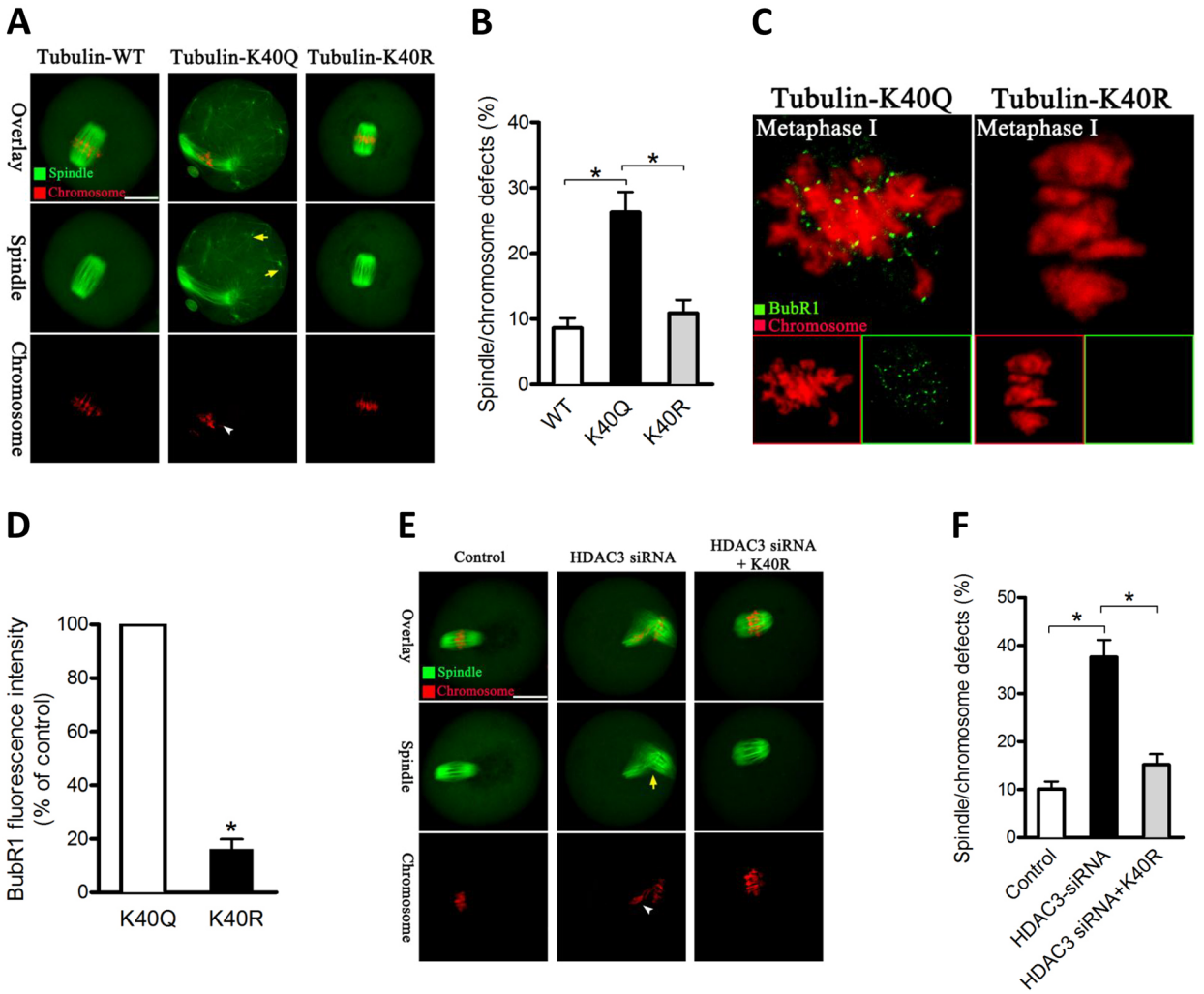

Fig. 8. Hypoacetylation of tubulin K40 is essential for spindle assembly and chromosome organization in mouse oocytes. (A) mRNA encoding Tubulin-WT, tubulin-K40Q or tubulin-K40R was injected into oocytes to evaluate the effects on spindle assembly and chromosome organization. Representative confocal images are shown. Arrowheads point to the misaligned chromosomes and arrowhead indicates the disorganized spindle. (B) Quantitative analysis of spindle and chromosome defects in oocytes injected with tubulin-WT (*n*=36), tubulin-K40Q (*n*=40) or tubulin-K40R (*n*=42). (C) Tubulin-K40Q and tubulin-K40R mutant mRNAs were injected into oocytes to evaluate their effects on SAC. Representative confocal images are shown. (D) Quantitative analysis of BubR1 fluorescence intensity in oocytes injected with tubulin-K40Q (*n*=24) or tubulin-K40R (*n*=26). (E) Representative images of meiotic spindle and chromosomes at metaphase in control oocytes, HDAC3 KD oocytes, and HDAC3 KD oocytes injected with tubulin-K40R mRNA. (F) Quantification of control (*n*=46), HDAC3 KD (*n*=48), and HDAC3 KD plus tubulin-K40R (*n*=52) oocytes with spindle/chromosome defects. Mean percentage±s.d. of three independent experiments. *P<0.05 versus controls. Scale bars: 30 µm.

anti-α-tubulin (F2168) antibodies (Sigma, 76074; 1:300). Secondary antibodies: Cy5-conjugated donkey anti-human IgG (709-605-149) and FITC-conjugated donkey anti-goat IgG (705-095-147) antibodies (Jackson ImmunoResearch Laboratories; 1:500); FITC-conjugated goat anti-rabbit IgG (ZSGB-BIO, China, ZF-0311) and TRITC-conjugated goat anti-rabbit IgG (ZSGB-BIO, China, ZF-0316) antibodies (Thermo Fisher Scientific; 1:300).

Oocyte collection and culture

At 46-48 h after injection of 5 IU pregnant mare serum gonadotropin (PMSG), fully grown cumulus-enclosed oocytes were collected from ovaries of 6- to 8-week-old female ICR mice. To obtain denuded oocytes, cumulus cells were removed by repeatedly pipetting. For *in vitro* maturation, oocytes were cultured in M16 medium under mineral oil at 37°C in a 5% CO_2 incubator.

Plasmid construction and mRNA synthesis

Total RNA was extracted from 50 denuded oocytes using the Arcturus PicoPure RNA Isolation Kit (Applied Biosystems), and cDNA was generated with the QIAquick PCR Purification Kit (Qiagen). Purified PCR products were digested with *Fse*I and *Asc*I (NEB) and cloned into the pCS2$^+$ vector with Myc tags. The vectors encoding the Myc-tubulin substitution mutants (K40Q and K40R) were generated with the QuikChange Site-Directed Mutagenesis Kit (Stratagene).

For the synthesis of mRNA, the HDAC3/tubulin-pCS2$^+$ plasmids were linearized by *Not*I. The capped cRNAs were *in vitro* transcribed with SP6 mMESSAGE mMACHINE (Ambion) and purified using the RNeasy Micro Kit (Qiagen) according to the manufacturer's instructions. Primers are listed in Table S1.

Knockdown and overexpression experiment

Microinjections of siRNA or mRNA with a Narishige microinjector were used to knock down or overexpress proteins in mouse oocytes, respectively. 2.5 pl 1 mM HDAC3 siRNA (5′-GACGGUACUAAAGUCACCUTT-3′; 5′-AGGUGACUUUAGUACCGUCTT-3′) was injected into oocytes for knockdown analysis, or an equivalent amount of negative siRNA (5′-UUCUCCGAACGUGUCACGUTT-3′; 5′-ACGUGACACGUUCGGAGAATT-3′; no significant sequence similarity to mouse, rat or human gene sequences) was injected as control. 10 pl mRNA solution (10 ng/µl) was injected into

Development (2017) 144, 3789-3797 doi:10.1242/dev.153353

oocytes for overexpression analysis, with RNase-free PBS injected as control. After injection, oocytes were arrested at GV stage in medium with 2.5 μM milrinone for 20 h, and then were cultured in milrinone-free medium for maturation.

Immunofluorescence

Oocytes were fixed in 4% paraformaldehyde for 30 min and permeabilized with 0.5% Triton X-100 for 20 min. After three washes, oocytes were blocked in 1% BSA in PBS for 1 h at room temperature. Sample were incubated overnight at 4°C with primary antibodies and then at room temperature for 1 h with secondary antibodies. To examine kinetochores, oocytes were colabeled with CREST antibody. Chromosomes were counterstained with Hoechst 33342 (blue, 1:300) or propidium iodide (red, 1:200) for 10 min. Oocyte samples were mounted on anti-fade medium (Vectashield) and examined under an LSM 710 laser scanning confocal microscope (Zeiss) equipped with 40× or 63× oil objectives. ImageJ software (National Institutes of Health) was used to quantify the intensity of fluorescence.

Quantitative real-time PCR (qRT-PCR)

qRT-PCR was performed as described previously (Hou et al., 2015). Total RNA was isolated from 50 oocytes and cDNA was quantified using an ABI StepOnePlus Real-Time PCR System (Applied Biosystems). The fold change in gene expression was calculated using the ΔΔCt method with the housekeeping gene glyceraldehydes-3-phosphate dehydrogenase (*Gapdh*) as the internal control. The result was expressed as fold change relative to control. Primers are listed in Table S2.

Western blotting

One hundred oocytes were lysed in Laemmli sample buffer containing protease inhibitor at 100°C for 5 min. Proteins were separated by 10% SDS-PAGE, transferred to PVDF membranes by constant current at 60 V, and then blocked in PBST (PBS containing 0.1% Tween 20) with 5% fat-free milk for 1 h at room temperature. Membranes were then incubated with rabbit anti-HDAC3 antibody (1:300; Santa Cruz, sc-376957) overnight at 4°C. After three washes in PBST and incubation with anti-rabbit horseradish peroxidase-conjugated secondary antibodies (ZSGB-BIO, China, ZB-2301; 1:2000), the protein bands were analyzed with an ECL Plus Western Blotting Detection System. The membrane was reprobed with anti-β-actin antibody (Sigma, A5441; 1:5000) to provide a loading control.

Chromosome spread

Chromosome spreading was conducted as previously described (Wang et al., 2009). Oocytes were exposed to Tyrode's buffer (pH 2.5) to remove the zona pellucida, and then fixed in a drop of 1% paraformaldehyde with 0.15% Triton X-100 on a glass slide. Samples were labeled with CREST antibody (1:500) for 1 h to detect kinetochores, and chromosomes were counterstained with Hoechst 33342 (1:300). The laser scanning confocal microscope was used to examine chromosome numbers in oocytes.

Statistical analysis

Data are presented as mean±s.d. unless otherwise stated. Differences between two groups were analyzed by Student's *t*-test. Multiple comparisons between more than two groups were analyzed by one-way ANOVA using Prism 5.0 (GraphPad). $P<0.05$ was considered significant.

Competing interests

The authors declare no competing or financial interests.

Author contributions

Conceptualization: X. Li, B.X., S.-C.S., H.L., L.G.; Methodology: X. Li, X. Liu, L.H., H.W.; Formal analysis: X. Li, X. Liu, M.G., D.Q., L.G.; Data curation: X. Li, H.W.; Writing - original draft: X. Li, L.G.; Writing - review & editing: B.X., S.-C.S., H.L., L.G.; Supervision: L.G.; Project administration: L.G.; Funding acquisition: L.G.

Funding

This work was supported by National Natural Science Foundation of China (31771660 and 31401227) and the Fundamental Research Funds for the Central Universities (KJQN201519).

Supplementary information

Supplementary information available online at
http://dev.biologists.org/lookup/doi/10.1242/dev.153353.supplemental

References

Bacon, T., Seiler, C., Wolny, M., Hughes, R., Watson, P., Schwabe, J., Grigg, R. and Peckham, M. (2015). Histone deacetylase 3 indirectly modulates tubulin acetylation. *Biochem. J.* **472**, 367-377.

Bhaskara, S., Knutson, S. K., Jiang, G., Chandrasekharan, M. B., Wilson, A. J., Zheng, S., Yenamandra, A., Locke, K., Yuan, J.-L., Bonine-Summers, A. R. et al. (2010). Hdac3 is essential for the maintenance of chromatin structure and genome stability. *Cancer Cell* **18**, 436-447.

Chen, Y.-T., Chen, Y.-F., Chiu, W.-T., Liu, K.-Y., Liu, Y.-L., Chang, J.-Y., Chang, H.-C. and Shen, M.-R. (2013). Microtubule-associated histone deacetylase 6 supports the calcium store sensor STIM1 in mediating malignant cell behaviors. *Cancer Res.* **73**, 4500-4509.

Duncan, F. E., Chiang, T., Schultz, R. M. and Lampson, M. A. (2009). Evidence that a defective spindle assembly checkpoint is not the primary cause of maternal age-associated aneuploidy in mouse eggs1. *Biol. Reprod.* **81**, 768-776.

Eddé, B., Rossier, J., Le Caer, J. P., Berwald-Netter, Y., Koulakoff, A., Gros, F. and Denoulet, P. (1991). A combination of posttranslational modifications is responsible for the production of neuronal α-tubulin heterogeneity. *J. Cell. Biochem.* **46**, 134-142.

Gal, J., Chen, J., Barnett, K. R., Yang, L., Brumley, E. and Zhu, H. (2013). HDAC6 regulates mutant SOD1 aggregation through two SMIR motifs and tubulin acetylation. *J. Biol. Chem.* **288**, 15035-15045.

Haberland, M., Montgomery, R. L. and Olson, E. N. (2009). The many roles of histone deacetylases in development and physiology: implications for disease and therapy. *Nat. Rev. Genet.* **10**, 32-42.

Horiuchi, M., Morinobu, A., Chin, T., Sakai, Y., Kurosaka, M. and Kumagai, S. (2009). Expression and function of histone deacetylases in rheumatoid arthritis synovial fibroblasts. *J. Rheumatol.* **36**, 1580-1589.

Hou, X., Zhang, L., Han, L., Ge, J., Ma, R., Zhang, X., Moley, K., Schedl, T. and Wang, Q. (2015). Differing roles of pyruvate dehydrogenase kinases during mouse oocyte maturation. *J. Cell Sci.* **128**, 2319-2329.

Ishii, S., Kurasawa, Y., Wong, J. and Yu-Lee, L.-Y. (2008). Histone deacetylase 3 localizes to the mitotic spindle and is required for kinetochore-microtubule attachment. *Proc. Natl. Acad. Sci. USA* **105**, 4179-4184.

Jiang, Y. D. and Hsieh, J. (2014). HDAC3 controls gap 2/mitosis progression in adult neural stem/progenitor cells by regulating CDK1 levels. *Proc. Natl. Acad. Sci. USA* **111**, 13541-13546.

Lane, S. I. R., Chang, H.-Y., Jennings, P. C. and Jones, K. T. (2010). The Aurora kinase inhibitor ZM447439 accelerates first meiosis in mouse oocytes by overriding the spindle assembly checkpoint. *Reproduction* **140**, 521-530.

Li, L. and Yang, X.-J. (2015). Tubulin acetylation: responsible enzymes, biological functions and human diseases. *Cell. Mol. Life Sci.* **72**, 4237-4255.

Ling, L., Hu, F., Ying, X., Ge, J. and Wang, Q. (2017). HDAC6 inhibition disrupts maturational progression and meiotic apparatus assembly in mouse oocytes. *Cell Cycle* (in press).

Ma, P. and Schultz, R. M. (2013). Histone deacetylase 2 (HDAC2) regulates chromosome segregation and kinetochore function via H4K16 deacetylation during oocyte maturation in mouse. *PLoS Genet.* **9**, e1003377.

Ma, P., Pan, H., Montgomery, R. L., Olson, E. N. and Schultz, R. M. (2012). Compensatory functions of histone deacetylase 1 (HDAC1) and HDAC2 regulate transcription and apoptosis during mouse oocyte development. *Proc. Natl. Acad. Sci. USA* **109**, E481-E489.

Ma, R., Hou, X., Zhang, L., Sun, S.-C., Schedl, T., Moley, K. and Wang, Q. (2014). Rab5a is required for spindle length control and kinetochore-microtubule attachment during meiosis in oocytes. *FASEB J.* **28**, 4026-4035.

Mahlknecht, U., Hoelzer, D., Bucala, R. and Eric Verdin, E. (1999). Cloning and characterization of the murine histone deacetylase (HDAC3). *Biochem. Biophys. Res. Commun.* **163**, 482-490.

Nogales, E. (2000). Structural insights into microtubule function. *Annu. Rev. Biochem.* **69**, 277-302.

Overlack, K., Primorac, I., Vleugel, M., Krenn, V., Maffini, S., Hoffmann, I., Kops, G. J. P. L. and Musacchio, A. (2015). A molecular basis for the differential roles of Bub1 and BubR1 in the spindle assembly checkpoint. *eLife* **4**, e05269.

Piperno, G., LeDizet, M. and Chang, X. J. (1987). Microtubules containing acetylated alpha-tubulin in mammalian cells in culture. *J. Cell Biol.* **104**, 289-302.

Remsberg, J. R., Ediger, B. N., Ho, W. Y., Damle, M., Li, Z., Teng, C., Lanzillotta, C., Stoffers, D. A. and Lazar, M. A. (2017). Deletion of histone deacetylase 3 in adult beta cells improves glucose tolerance via increased insulin secretion. *Mol. Metab.* **6**, 30-37.

Santaguida, S. and Musacchio, A. (2009). The life and miracles of kinetochores. *EMBO J.* **28**, 2511-2531.

Schatten, G., Simerly, C., Asai, D. J., Szöke, E., Cooke, P. and Schatten, H. (1988). Acetylated α-Tubulin in microtubules during mouse fertilization and early development. *Dev. Biol.* **130**, 74-86.

Seto, E. and Yoshida, M. (2014). Erasers of histone acetylation: the histone deacetylase enzymes. *Cold Spring Harb. Symp.* **6**, 18713.

Development (2017) 144, 3789-3797 doi:10.1242/dev.153353

Takami, Y. and Nakayama, T. (2000). N-terminal region, C-terminal region, nuclear export signal, and deacetylation activity of histone deacetylase-3 are essential for the viability of the DT40 chicken B cell line. *J. Biol. Chem.* **275**, 16191-16201.

Tauchman, E. C., Boehm, F. J. and DeLuca, J. G. (2015). Stable kinetochore-microtubule attachment is sufficient to silence the spindle assembly checkpoint in human cells. *Nat. Commun.* **6**, 10036.

Vidal, M. and Gaber, R. F. (1991). RPD3 encodes a second factor required to achieve maximum positive and negative transcriptional states in Saccharomyces cerevisiae. *Mol. Cell. Biol.* **11**, 6317-6327.

Wang, Q., Ratchford, A. M., Chi, M. M.-Y., Schoeller, E., Frolova, A., Schedl, T. and Moley, K. H. (2009). Maternal diabetes causes mitochondrial dysfunction and meiotic defects in murine oocytes. *Mol. Endocrinol.* **23**, 1603-1612.

Yang, X.-J. and Seto, E. (2008). The Rpd3/Hda1 family of lysine deacetylases: from bacteria and yeast to mice and men. *Nat. Rev. Mol. Cell Biol.* **9**, 206-218.

Yang, W.-M., Yao, Y.-L., Sun, J.-M., Davie, J. R. and Seto, E. (1997). Isolation and characterization of cDNAs corresponding to an additional member of the human histone deacetylase gene family. *J. Biol. Chem.* **272**, 28001-28007.

Zhan, P., Wang, X., Liu, X. and Suzuki, T. (2017). Medicinal chemistry insights into novel HDAC inhibitors: an updated patent review. *Recent Pat. Anticancer Drug Discov.* **12**, 16-34.

Zhang, L., Han, L., Ma, R., Hou, X., Yu, Y., Sun, S., Xu, Y., Schedl, T., Moley, K. H. and Wang, Q. (2015). Sirt3 prevents maternal obesity-associated oxidative stress and meiotic defects in mouse oocytes. *Cell Cycle* **14**, 2959-2968.

Zhou, D., Choi, Y. J. and Kim, J. H. (2017). Histone deacetylase 6 (HDAC6) is an essential factor for oocyte maturation and asymmetric division in mice. *Sci. Rep.* **7**, 8131.

Zilberman, Y., Ballestrem, C., Carramusa, L., Mazitschek, R., Khochbin, S. and Bershadsky, A. (2009). Regulation of microtubule dynamics by inhibition of the tubulin deacetylase HDAC6. *J. Cell Sci.* **122**, 3531-3541.

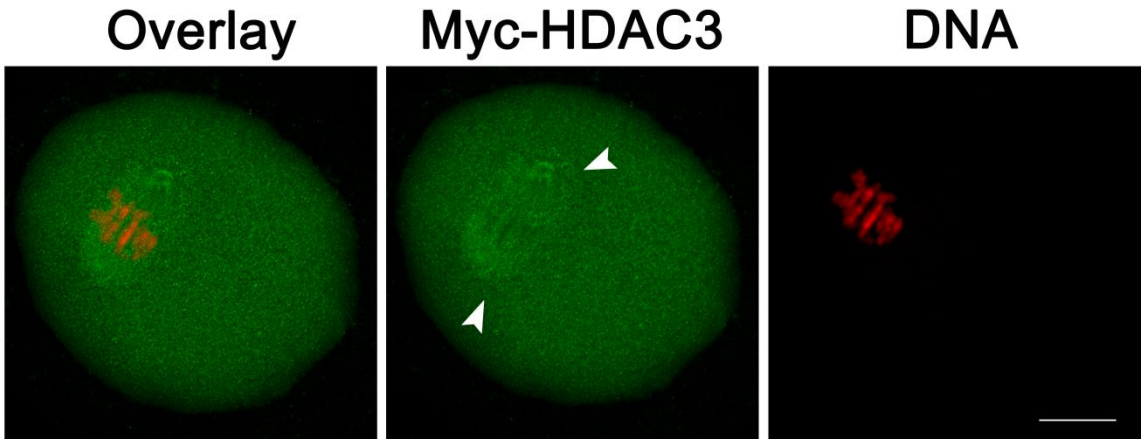

Figure S1 Localization of Myc-HDAC3 in mouse oocytes. Representative confocal sections showing the Myc-HDAC3 cRNA injected-oocytes stained with anti-Myc antibody (green) and counterstained with propidium iodide (red) for chromosomes. Scale bar, 20 µm.

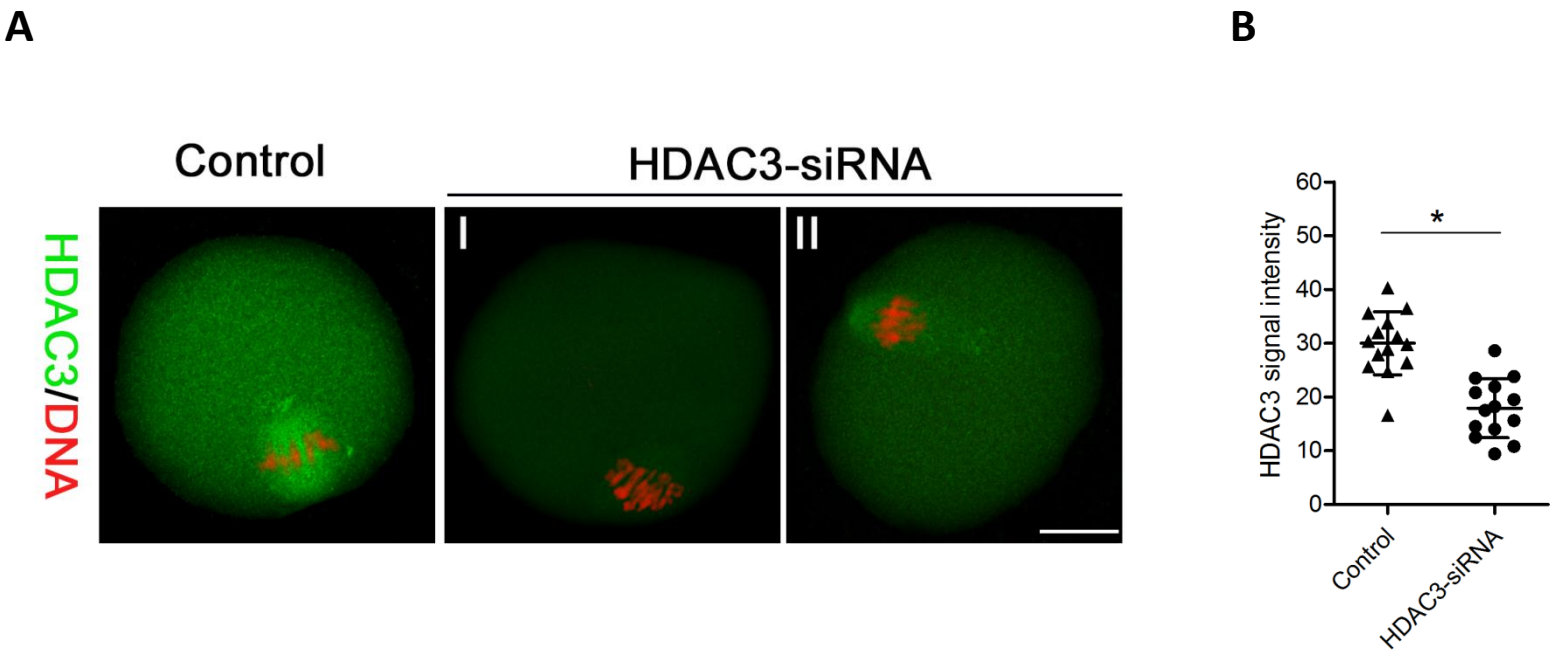

Figure S2 Effects of siRNA knockdown on HDAC3 staining in oocytes. (A) Representative confocal sections of control and HDAC3-siRNA injected oocytes stained with anti-HDAC3 antibody (green) and counterstained with propidium iodide (red) for nuclear are shown. Scale bar, 20 µm. (B) Quantification of HDAC3 immunofluorescence shown in A (n = 14 for control and n = 14 for HDAC3-siRNA group). Results are mean ± SD from three independent experiments. *, P < 0.05.

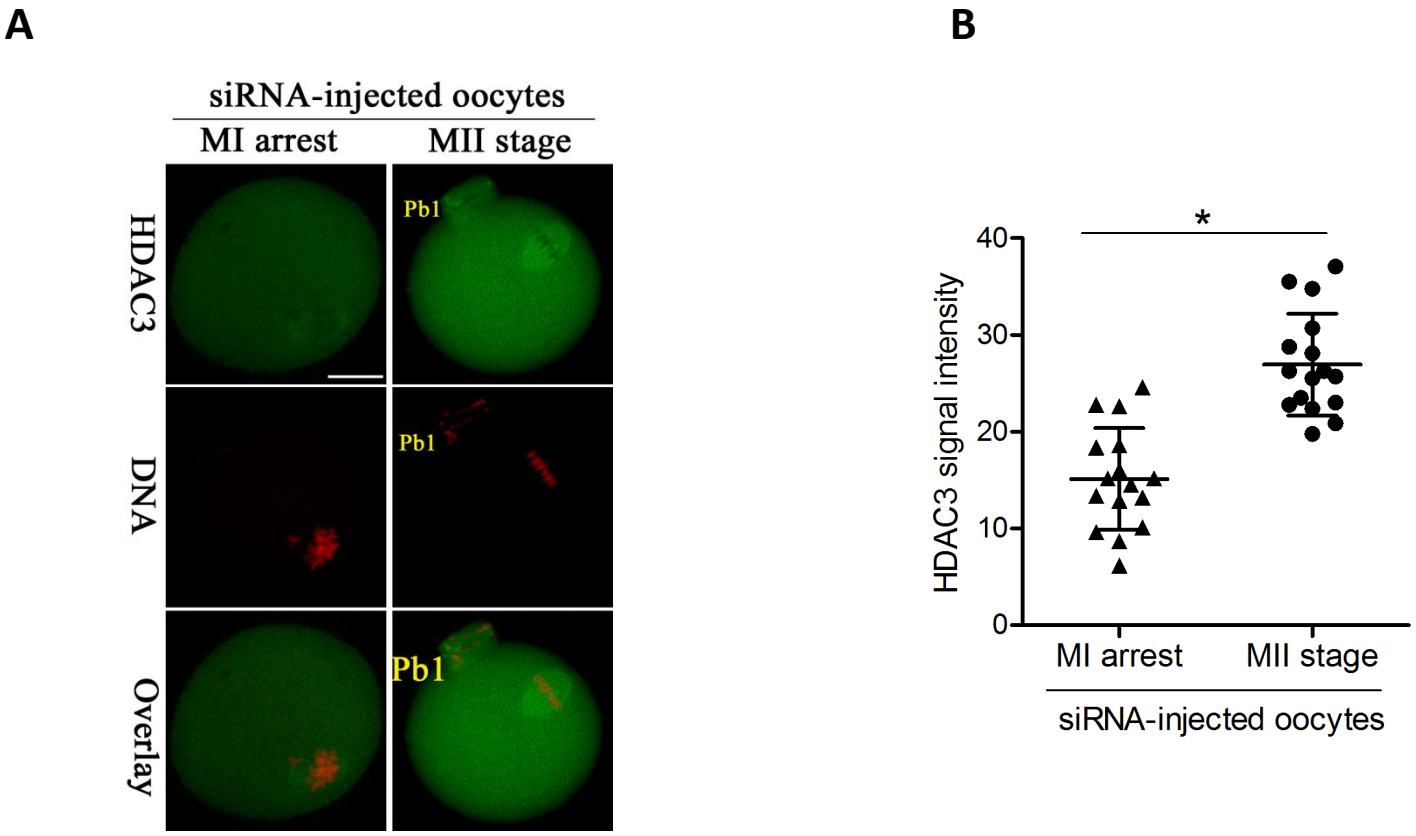

Figure S3 HDAC3 staining in siRNA-injected oocytes with or without first polar body. (A) Representative confocal sections of MI arrest and MII stage oocytes stained with anti-HDAC3 antibody (green) and counterstained with propidium iodide (red) for nuclear are shown. Pb1. first polar body. Scale bar, 20 µm. (B) Quantification of HDAC3 immunofluorescence shown in A (n = 15 for MI arrest oocytes and n = 15 for MII stage oocytes). Results are mean ± SD from three independent experiments. *, P < 0.05.

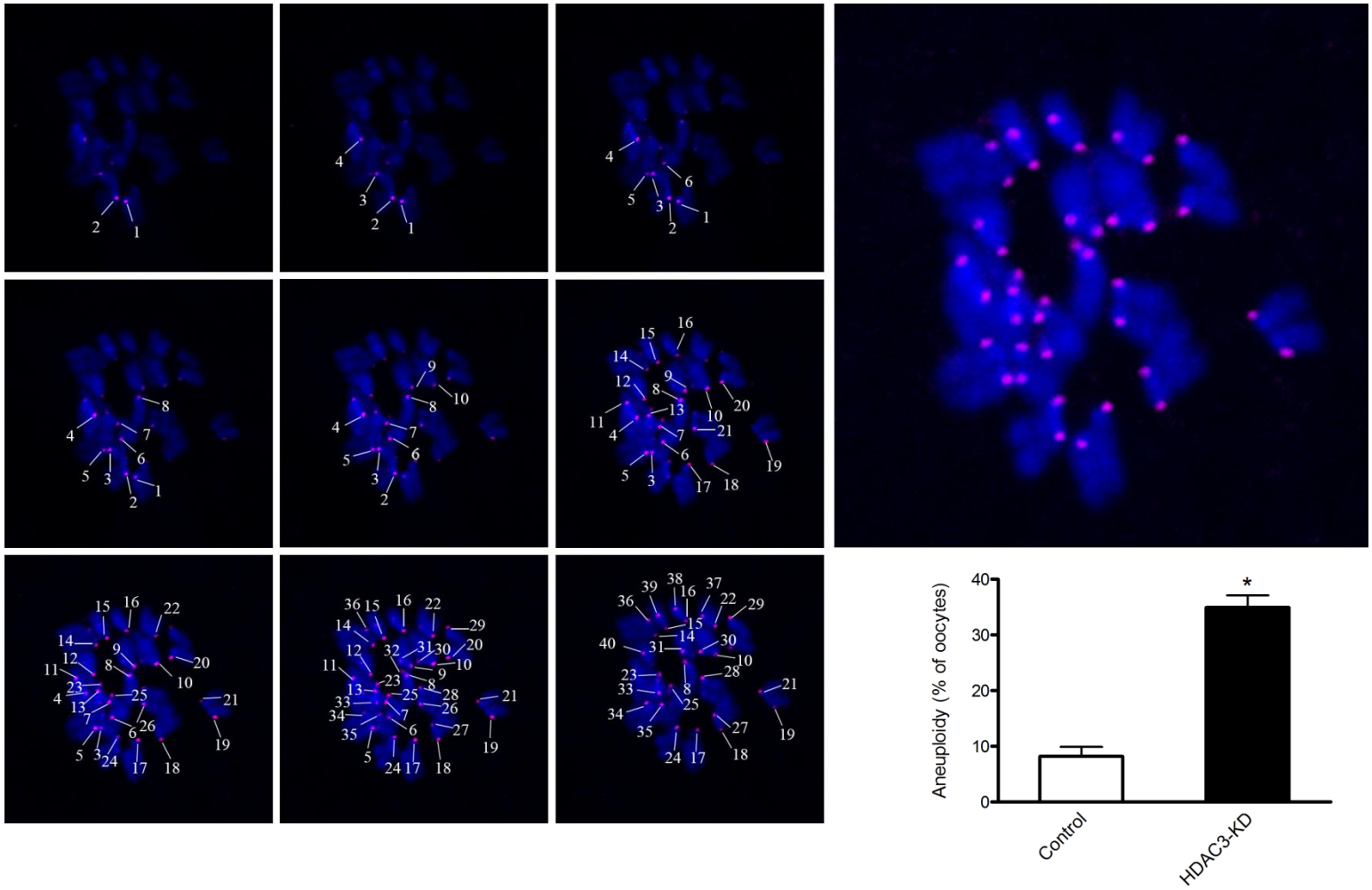

Figure S4 Chromosome counts with a monastrol-based in situ spreading technique. (A) The inset shows a flattened Z-stack series of images through a monastrol-treated oocyte; kinetochores are shown in purple and chromosome (Hoechst) in blue. The left panel shows the individual Z-planes from which the inset is comprised; 40 CREST-positive foci are counted in an euploid oocyte. (B) Proportion of aneuploidy in control and HDAC3-KD oocytes. Results are mean ± SD from three independent experiments. *, P < 0.05.

Table S1 Primer sequences of genes for cDNA amplification and mutant construction

Gene	***Primer sequence***
HDAC3	Forward primer: 5′-GGGGGCCGGCCCCATGGCCAAGACCGTGG-3′
	Reverse primer:5′-GGGGGCGCGCCGGGGAAGAGGGGCTGAGG-3′
α-Tubulin	Forward primer:5′-GGG GGCCGGCCATGCGTGAGTGCATCTCC -3′
	Reverse primer:5′-GGGGGCGCGCCCACAATAAACATCCCTGTGG-3′
Tubulin-K40R	Forward primer:5′-CAGATGCCAAGTGACAGGACCATTGGGGGA-3′
	Reverse primer: 5′-CTGTCACTTGGCATCTGGCCATCAGGC-3′
Tubulin-K40Q	Forward primer:5′-CAGATGCCAAGTGACCAGACCATTGGGGGA-3′
	Reverse primer: 5′-GGTCACTTGGCATCTGGCCATCAGGC-3′

Table S2 Primer sequences of genes for qRT-PCR

Gene	***Primer sequence***
GAPDH	Forward Primer: 5’ –CTTTGTCAAGCTCATTTCCTGG – 3’
	Reverse Primer: 5’ –TCTTGCTCAGTGTCCTTGC – 3’
HDAC3	Forward primer, 5’-GCCAAGACCGTGGCGTATT-3’
	Reverse primer, 5’- GTCCAGCTCCATAGTGGAAGT-3’